

SUPPLEMENTARY INFORMATION

G-749, a novel FLT3 kinase inhibitor can overcome drug resistance for the treatment of Acute Myeloid Leukemia

Hee Kyu Lee¹, Hong Woo Kim², In Yong Lee², Jaekyoo Lee², Jungmi Lee², Dong Sik Jung¹, Sang Yeop Lee¹, Sung Ho Park¹, Haejun Hwang¹, Jang-Sik Choi¹, Jung-Ho Kim¹, Se Won Kim¹, Jung Keun Kim¹, Jan Cools³, Jong Sung Koh², and Ho-Juhn Song^{2*}

¹Oscotec Inc., Korea Bio-Park, 694-1, Sampyeong-dong, Bundang-gu, Seongnam-si, Gyeonggi-do, 463-400 Republic of Korea; ² Genosco, 767C Concord Ave, Cambridge, MA 02138, USA; ³ Center for the Biology of Disease, VIB, Leuven, Belgium

*Corresponding author:

Ho-Juhn Song, Ph.D.
767C Concord Avenue
Cambridge, MA 02138
U.S.A.

Email) hsong@genosco.com

Phone) 1-617-494-1460

Supplementary Methods

Synthetic process of G-749

Preparation of ethyl 4-methyl-2-methylthio-6-(4-phenoxy-phenylamino)pyrimidine-5-carboxylate (2) 50 mL of concentrated HCl was added to a solution of 5.0 kg of **1** (19.3 mol, 1.0 equiv.) and 3.57 kg of 4-phenoxyaniline (19.3 mol, 1.0 equiv.) in 35 L of ethanol, and the reaction mixture was heated to reflux for 3 h. The reaction mixture was concentrated after TLC indicated that starting material was consumed. The residue was diluted with 20 L of methylene chloride, washed with 20 L of water, and the aqueous layer was extracted with 5 L of methylene chloride. The combined organic layer was washed with 8 L of saturated aqueous NaHCO₃ and 5 L of brine, dried with Na₂SO₄ and then concentrated under reduced pressure. The resulting residue was triturated in 4 L of t-butylmethylether. The white solids were collected by filtration to give 6.7 kg of **2**, yielding 96.8%.

¹HNMR (400 MHz, CDCl₃) δ (ppm): 10.58 (s, 1H), 7.59-7.62 (m, 2H), 7.34-7.38 (m, 2H), 7.08-7.12 (m, 1H), 7.0-7.08 (m, 4H), 4.40-4.46 (q, J = 7.12 Hz, 2H), 2.67 (s, 3H), 2.51 (s, 3H), 1.44-1.47 (t, J = 7.12 Hz, 3H).

Preparation of 2-methylthio-4-(4-phenoxy-phenylamino)-6H-pyrido[4,3-d]pyrimidin-5-one (4) A mixture of 2.25 kg of **2** (5.6 mol, 1.0 equiv.) and 800 g of DMF-DMA (7.2 mol, 1.3 equiv.) in 5.5 L of DMF was heated to 120~126 °C for 3h. The reaction mixture was concentrated under reduced pressure, and the residue was solidified by addition of 4 L of t-butylmethylether. The resulting yellow solids were collected and dried to give 2.5 kg of a inseparable mixture of **3a** and **3b** (1:1.5) yielding 97%. A mixture of 800 g of the mixture of **3a** and **3b**, 800 mL of 28% ammonium hydroxide and 7 L of ethanol were charged into 10 L autoclave and the mixture was heated at 95 °C for 6 h. After cooling down to 20 °C, the resulting yellow solids were collected, washed with 500 mL of ethanol and then dried to give 521 g of **4**, yielding 75.1%.

¹H NMR (400 MHz, DMSO-d₆) δ (ppm): 11.94 (s, 1H), 11.92 (bs, 1H), 7.76 (d, J = 8.96 Hz, 2H), 7.56 (d, J = 7.25 Hz, 1H), 7.39 (dd, J₁ = 7.64 Hz, J₂ = 8.36 Hz, 1H), 7.13 (t, J = 7.36 Hz, 1H), 7.05 (d, J = 8.96 Hz, 2H), 7.02 (d, J = 7.76 Hz, 2H), 6.32 (d, J = 7.20 Hz, 1H), 2.50 (s, 3H).

Preparation of 8-bromo-2-methylthio-4-(4-phenoxy-phenylamino)-6H-pyrido[4,3-d]pyrimidin-5-one (5) A suspension of 800 g of **4** (2.12 mol, 1.0 equiv.) in 8 L of DMF was heated at 80 °C to give a clear solution. After being cooled to 60 °C, NBS (378 g, 2.12 mol, 1.0 equiv.) was added in aliquots into the solution, and the reaction mixture was stirred further at 65 °C for 17 h. The reaction mixture was allowed to cool to 50 °C to form solids. The resulting solids were collected by filtration, washed with 2L of ethanol and dried to give 720 g of **5** as a yellow solid, yielding 74.5%.

¹H NMR (400M Hz, d₆-DMSO) δ (ppm) 12.30 (d, J = 6.44Hz, 1H), 12.01 (s, 1H), 8.02 (d, J = 6.40Hz, 1H), 7.76 (d, J = 6.40Hz, 2H), 7.40 (m, 2H), 7.16(m, 1H), 7.02-7.08 (m, 4H), 2.51 (s, 3H).

Preparation of 8-bromo-2-(1-methyl-piperidin-4-ylamino)-4-(4-phenoxyphenylamino)-6H-pyrido[4,3-d]pyrimidin-5-one (6) Compound **5** (328.4 g, 1 equiv.) was added into a 10L reactor containing 3.5L DMF. m-CPBA (372.4 g, 3 equiv.) was added portionwise with controlling reaction temperature below 30 °C with ice water. After 2h, LC/MS indicated no starting material left. Triethylamine (218.6 g, 3 equiv.) was then slowly added. After stirring for 10min, N-methyl-4-aminopiperidine (112.5 g, 1.5 equiv.) was added and the reaction mixture was stirred overnight at room temperature. Additional N-Methyl-4-aminopiperidine (35 g, 0.5 equiv.) was added and the reaction mixture was heated to 40-50 °C for 1h. Reaction mixture was concentrated and methylene chloride (6L) was added into the residue. The organic layer was washed with saturated sodium carbonate (3L*2), followed by brine (4L). The separated organic layer was stood to form precipitate. After sitting for 12h at rt, the solids were collected by filtration and then recrystallized from mixture of THF : EtOH = 1 : 12 to provide 200g of off-white solid **6**, yielding 52.3%.

¹H NMR (400M Hz, CDCl₃) δ (ppm): 11.62 (s, 0.7H), 11.42 (s, 0.3H), 11.09 (br s, 1H), 7.70-7.79 (m, 2H), 7.56 (m, 1H), 7.32-7.39 (m, 2H), 7.02-7.14 (m, 5H), 5.79 (d, J = 7.32Hz, 0.7H), 5.43 (d, J = 7.04Hz, 0.3H), 3.88 (m, 0.3H), 3.75 (m, 0.7H), 2.90 (m, 2H), 2.01-2.37 (m, 7H), 1.66 (m, 2H).

Kinase assays

Activity assays were conducted using Lance Ultra time-resolved fluorescence resonance energy transfer (TR-FRET) technology from Perkin-Elmer. Briefly, 10 ng/ml FLT3 enzyme, a serial diluted G-749, 80 nM substrate of ULight-poly-GT peptide and variable amounts of ATP (8.5 μM to 1088 μM) were mixed in kinase assay buffer (50 mM HEPES pH 7.5, 10 mM MgCl₂, 1 mM EGTA, 2 mM DTT and 0.01% Tween-20) and were added to a 384-well OptiPlate-384 in a volume of 10 μL. Kinase reactions were incubated at room temperature for upto 1 h and then stopped by the addition of 5 μL of 10 mM EDTA. A volume of 5 μL of the specific Eu-labeled-anti-phosphopeptide antibody diluted in LANCE Detection Buffer was then added to a final concentration of 2 nM. After 30-minute incubation, assay plates were incubated at 23°C and the LANCE signal was measured on an EnVision Multilabel Reader (Perkin-Elmer). Excitation wavelength was set at 320 nm and emission monitored at 615 nm (donor) and 665 nm (acceptor). The IC₅₀ was calculated using nonlinear regression analysis by GradPad Prism 5.

Western Blot analysis

AML cell lines, BaF3 FLT3 mutant cells or human patient primary cells were treated with the indicated concentration of FLT3 inhibitors for 2 hours. For FL addition experiment, Molm-14 and RS4-11 cells were stimulated with 50 ng/mL FLT3 ligand (Invitrogen) for 5 minutes. Cells were lysed in RIPA buffer (25mM Tris•HCl pH 7.6, 150mM NaCl, 1% NP-40, 1% sodium deoxycholate, 0.1% SDS) containing protease and phosphatase inhibitor cocktail (Thermo scientific). Equivalent amounts of protein were separated by NuPAGE 4–12% Bis-Tris Gel system (Invitrogen), and then transferred to polyvinylidene difluoride membranes. Membranes were probed with an anti-phospho-FLT3 antibody (Cell Signaling Technology) and then stripped with Restore Western Blot Stripping Buffer (Thermo Scientific). Membranes were probed again with an anti-FLT3 antibody (Santa Cruz

Biotechnology). The membranes were visualized by enhanced chemilluminescence. To examine the phosphorylation levels of STAT5, ERK1/2, AKT and Foxo3a, the same whole cell lysates were subjected to immunoblotting with anti-phospho-STAT5, phospho-ERK1/2, phospho-AKT antibodies and phosphor-Foxo3a (Cell Signaling Technology). Anti-STAT5, anti-ERK1/2, anti-AKT, anti-Foxo3a and anti-PARP antibodies were purchased from Cell Signaling Technology. The PIA assay was performed as previously described^{16,44}. Normal human plasma was obtained from Sigma-Aldrich. AML patient plasmas with relapse or remission were obtained from Seoul National University Hospital (Seoul, S. Korea).

Immunoprecipitation

After incubation with drugs, cells were harvested, washed with ice-cold PBS and lysed with cell lysis buffer (150 mM NaCl, 1.5 mM MgCl₂, 50 mM HEPES pH 7.5, 10% glycerol, 1.0% Triton X-100, 1 mM EGTA, 50 mM NaF, 1 mM Na₃VO₄) containing protease inhibitor cocktail (Thermo scientific). Protein content of the lysates was determined using the bicinchoninic acid assay (Bio-Rad, Hercules, CA). One mg of proteins was incubated with antibodies against human FLT3 (Santa Cruz Biotechnology) overnight at 4°C and additionally with Dynabeads-protein A (Invitrogen) for 2 hours at 4°C. After washing with cell lysis buffer three times, the immunoprecipitates were separated by NuPAGE 4-12% Bis-Tris Gel system (Invitrogen), and then transferred to polyvinylidene difluoride membranes. FLT3 phosphorylation was measured by probing with an anti-phosphotyrosine antibody (Millipore, 4G10). Proteins were detected using enhanced chemiluminescence and visualized after exposure to Kodak film. To verify equal loading, blots were stripped and reprobed with antibodies to anti-FLT3 (Santa Cruz Biotechnology) to measure total FLT3.

IL-3 rescue assay

The IL-3 rescue assay was performed as previously described (Keith, W. *et al Blood* **115**, 1425-1432 (2010)).

In vivo mouse models

Pharmacodynamic study: MV4-11 tumor model was established by subcutaneous injection (Sundia, China). Athymic nu/nu mice bearing tumors (approximate 450 mm³) were administered as a single oral dose of 10 mg/kg G-749 HCl salt. At the indicated time points, mice were sacrificed and then tumor tissues were freshly dissected and frozen in liquid nitrogen. Tumors were homogenized in ice-cold lysis buffer and centrifuged at 16,000 g for 10 minutes. The levels of FLT3 phosphorylation were measured by ELISA according to manufacturer's protocol. In parallel, tumor lysates were assayed for STAT5 and ERK1/2 phosphorylations by Western blotting.

Subcutaneous model: Athymic nu/nu mice were subcutaneously inoculated with MV4-11 cells (5 × 10⁶) (Sundia, China). When the average tumor volume reach approximately 500 mm³, G-749 HCl salt (3, 10 and 30 mg/kg/day) was orally and *quaque die* administered in a 20% hydroxypropyl-β-cyclodextrin (HPBCD) for 28 days. Tumor volume and body weight were measured with caliper twice weekly. Tumor volumes were calculated by the formula: Tumor volume = length × width² / 2.

Bone marrow engrafted model: NOD-SCID mice were pretreated with cyclophosphamide (Sigma-Aldrich) by intraperitoneal injection of 150 mg/kg/day for 2 days⁴⁵, followed by 24 hours of rest prior to intravenous injection of 5 × 10⁶ Molm-14 cells via the tail vein. G-749 HCl salt (10 and 20 mg/kg/day) and its vehicle were dosed daily by oral gavage. Survival was determined by observation when the animals demonstrated hind-limb paralysis and became moribund.

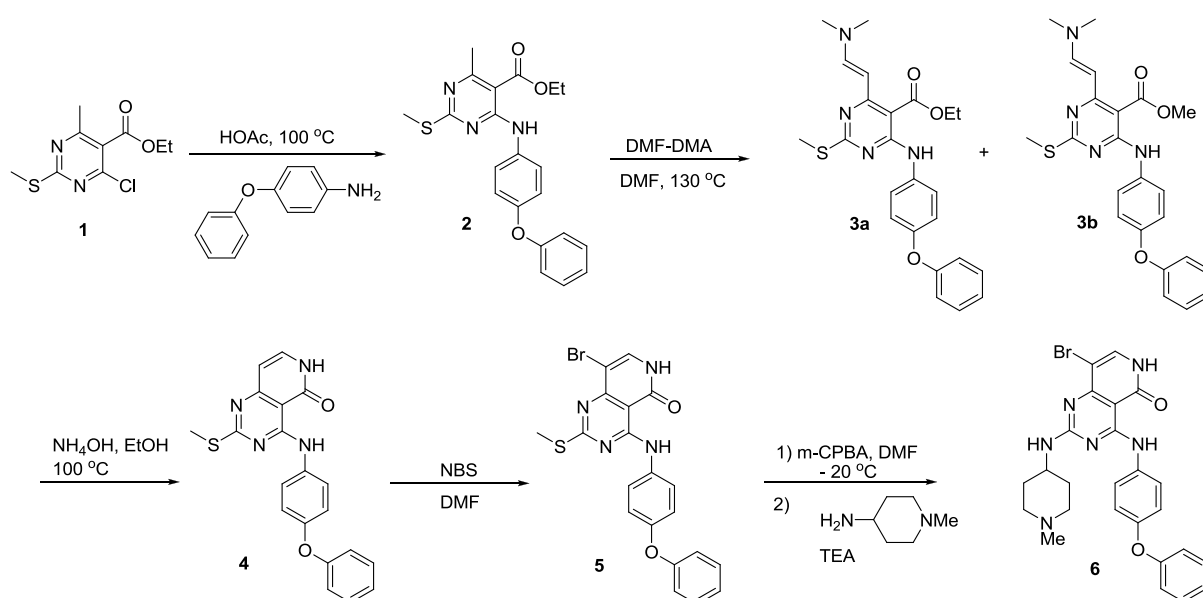
Statistical analysis

Analysis of variance (ANOVA) was performed by Prism 5.0 to examine whether the inhibition level of p-FLT3 in patient plasma milieu differs among compound treat group. The individual value at each test concentration was plotted as scatter plot to display distribution of data. Newman-Keuls Multiple Comparison Test method was performed to identify the pairs of test compounds with different inhibition levels. ANOVA followed by Dunnett's post-test was performed for analysis of tumor size. For disseminated mouse model, Kaplan-Meier curves were plotted and the log-rank (Mantel-Cox) test

was made for comparing two survival curves between vehicle treated group and 10 or 20 mg/kg/day group.

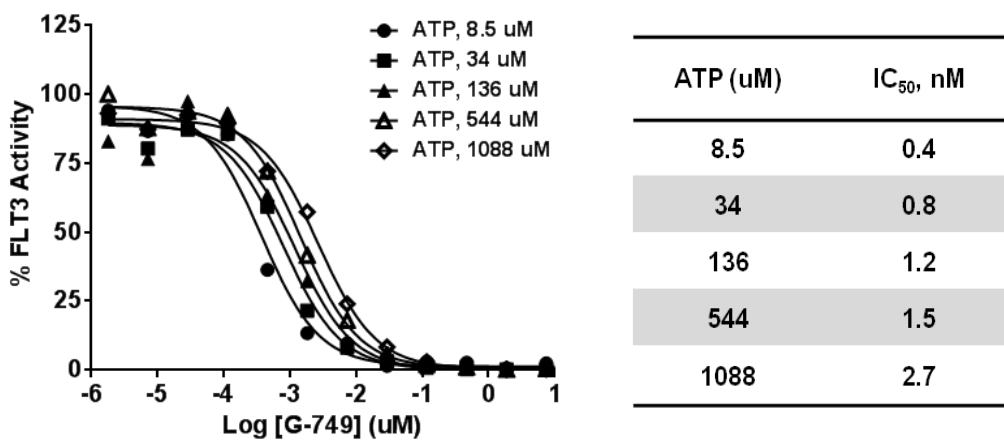
Supplementary Figures

Supplementary Figure 1.



Supplementary Figure 1. Related Figure 1a. Synthetic Route to G-749

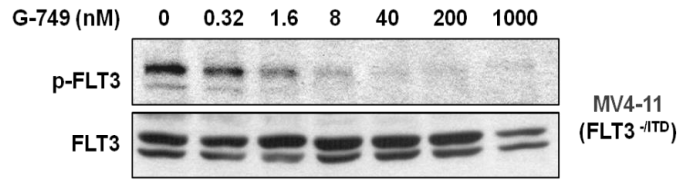
Supplementary Figure 2.



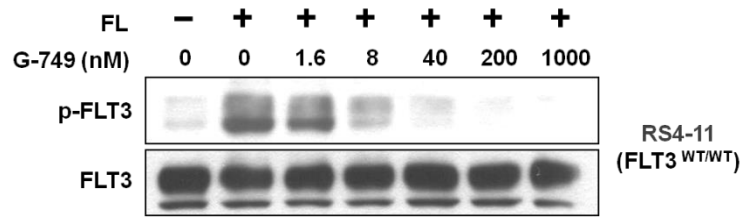
Supplementary Figure 2. Related Figure 1. ATP competition assay. A series of concentrations of G-749 ranging from 0.1 μ M to 30 μ M were simultaneously incubated with the indicated ATP concentrations ranging from app ATP Km to 1088 μ M, substrate of ULight-poly GT peptide and recombinant FLT3 enzyme. Phosphorylated peptide substrates were then incubated with Europium-labeled anti-phosphospecific antibodies and Europium was detected using time-resolved fluorescence. The results are presented as percentage of residual kinase activity relative to the DMSO control (graph). The IC₅₀ values at various ATP concentrations were calculated by non-linear regression curve and tabulated on right.

Supplementary Figure 3. Related Figure 1a.

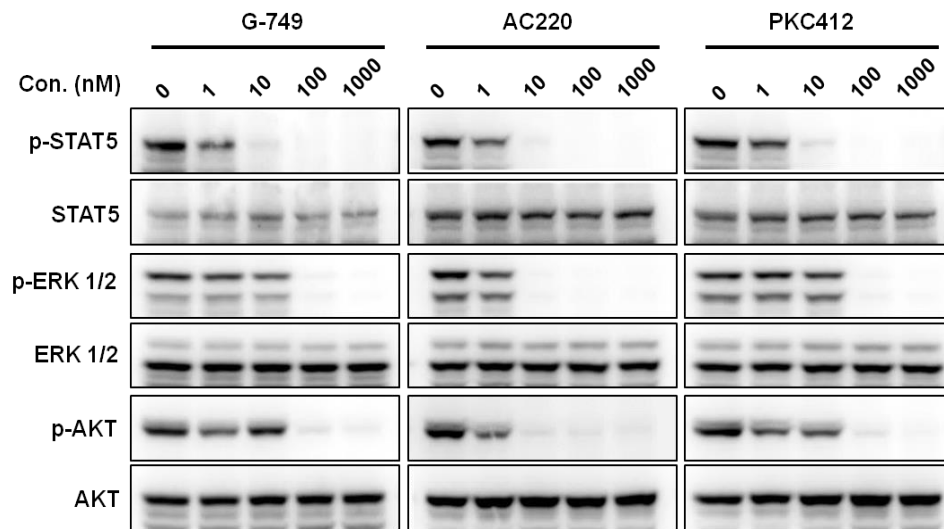
A



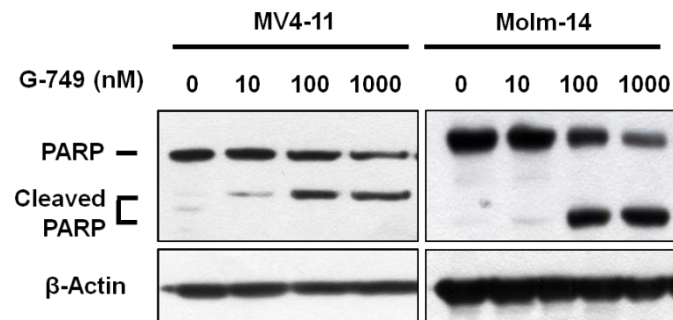
B



C

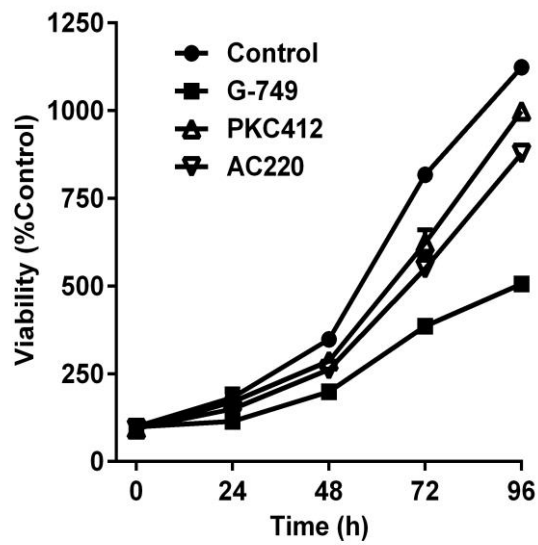


D



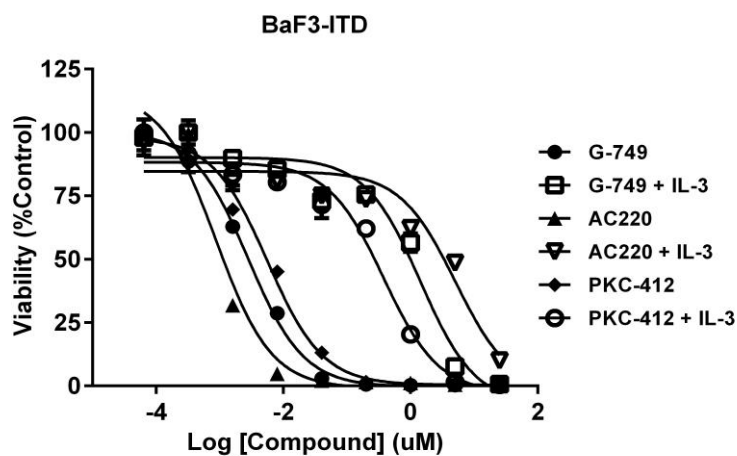
Supplementary Figure 3. Related Figure 1. (A) MV4-11 cells were incubated with the indicated concentrations of G-749 for 2 hr prior to cell lysis. Whole cell lysates were immunoprecipitated with anti-FLT3 antibody and then resolved by SDS-PAGE. Immunoblots were probed with anti-phosphotyrosine antibody. Membranes were stripped and reprobed with anti-FLT3 for loading control. (B) RS4-11 cells were incubated with the indicated concentrations of G-749 for 2 hr before being stimulated with 50 ng/mL of FLT3 ligand (FL) for 15 min. After cell lysis, FLT3 autophosphorylation was detected by immunoblotting. (C) For direct comparison of three inhibitors, MV4-11 cells were treated with the indicated concentrations of each inhibitor for 2 hr. The phosphorylation level of downstream effectors, such as STAT5 (Tyr 694), AKT (Ser 473) and ERK1/2 (Thy 202/Tyr 204), was then evaluated by immunoblotting. (D) MV4-11 and Molm-14 cells were incubated with various concentrations of G-749 for 24 hr and then the apoptosis signaling induced by G-749 was evaluated by immunoblotting using anti-PARP antibody.

Supplementary Figure 4.



Supplementary Figure 4. Related Figure 1. Prolonged inhibitory activity of G-749. MV4-11 cells were pre-incubated with 100 nM of the indicated FLT3 inhibitors for 2 hr and then washed two times with fresh medium. Then, equal numbers of cells were seeded into a 96 well plate and cultured for additional 96 hr. Cell growth was monitored using ATPLite assay at each indicated time point of 24, 48, 72 and 96 hr. Error bar shows S.D.

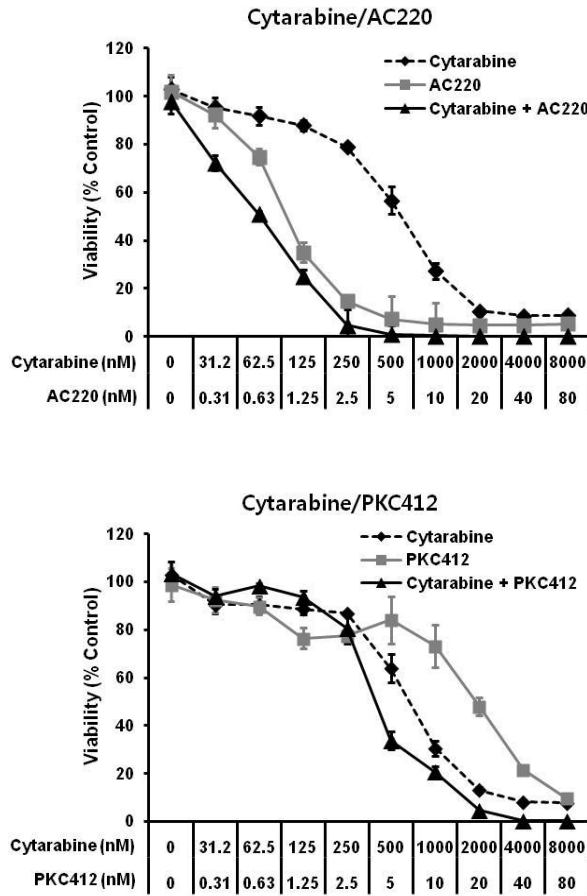
Supplementary Figure 5.



Compound	IC ₅₀	IL-3 IC ₅₀	Index
G-749	2.8	1426.0	509.3
AC220	0.9	5082.0	5646.7
PKC412	5.6	376.0	67.1

Supplementary Figure 5. Related Figure 1. IL-3 rescue assay. BaF3 cells expressing FLT3-ITD were exposed to increasing concentrations of FLT3 inhibitors in the presence or absence of IL-3 (1 ng/mL). After 72 hr incubation, ATPLite assay were carried out to determine the number of viable cells. The IL-3 index which is calculated by the ratio of the IC₅₀ in the presence of IL-3 divided by that in the absence of IL-3 was tabulated below the graphs.

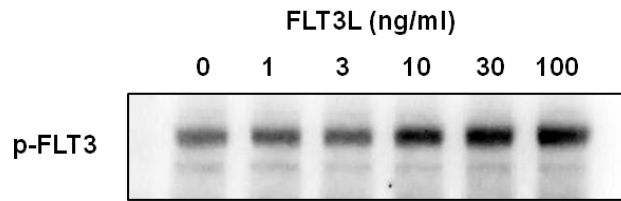
Supplementary Figure 6.



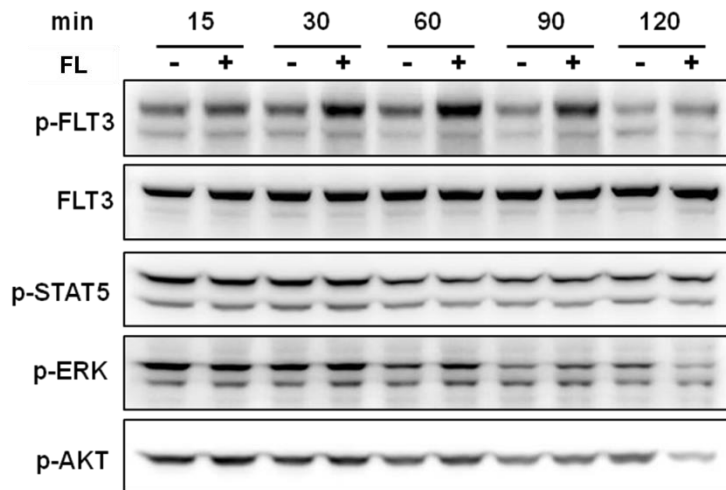
Supplementary Figure 6. Related to Figure 1. Cytotoxic response to FLT3 inhibitors in combination with standard cytotoxic agent, cytarabine. MV4-11 cells were simultaneously treated with cytarabine and AC220 or PKC412 for 72 hr and cell viability was counted by ATPLite assay. Representative results are shown from two independent experiments. Calcsyn analysis suggests that AC220 (ED_{50} : 0.50273; ED_{75} : 0.40505; ED_{90} : 0.32834) and PKC412 (ED_{50} : 0.91831; ED_{75} : 0.57967; ED_{90} : 0.37029) show moderate synergism. Note that G-749 also show moderate synergistic effect (ED_{50} : 0.58264; ED_{75} : 0.50659; ED_{90} : 0.44793).

Supplementary Figure 7

A

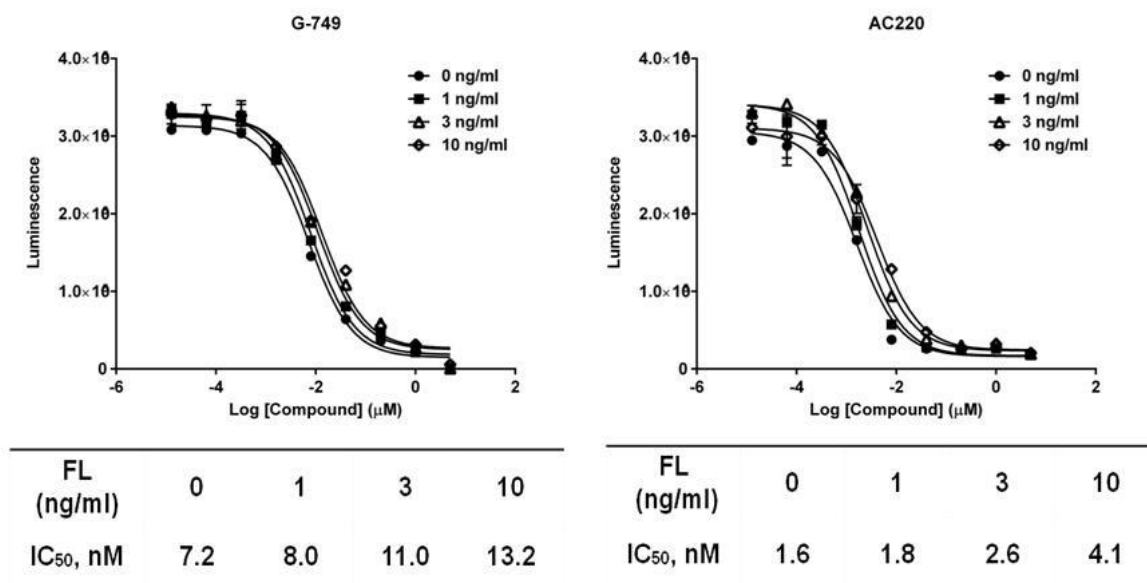


B



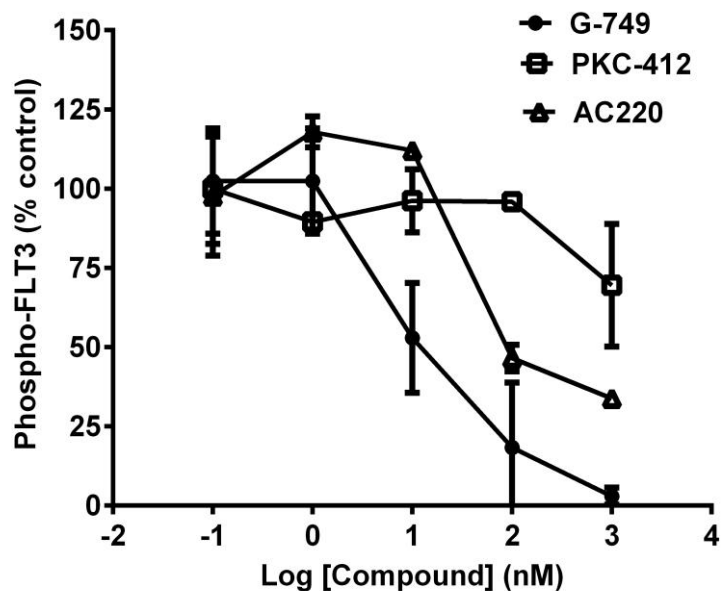
Supplementary Figure 7. Related to Figure 2. (A) BaF3 cells expressing wild type FLT3 were treated with the indicated concentrations of human FLT3 ligand (FL) for 1 hr. the FL-induced autophosphorylation of FLT3 was determined by immunoblotting. (B) BaF3 cells expressing wild type FLT3 were treated with 10 ng/mL FL and then harvested at the indicated time points. The phosphorylation levels of FLT3, STAT5, ERK and AKT were analyzed by immunoblotting. Note that p-STAT5 was unchanged in the absence or presence of FL. Noticeable changes in ERK and AKT activations were observed when FLT3 activation signal reached maximum at 60 min.

Supplementary Figure 8.



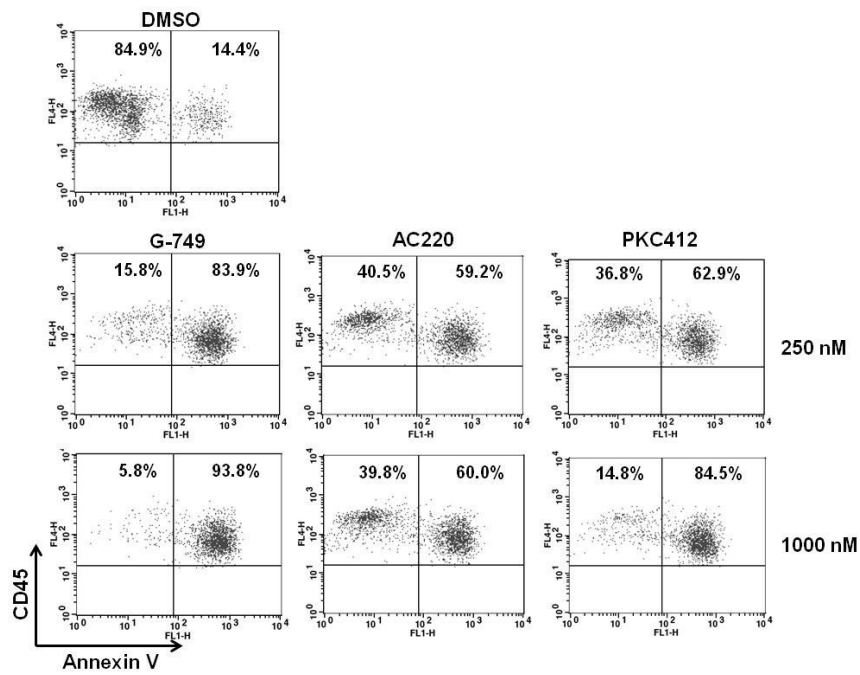
Supplementary Figure 8. Related to Figure 2. Molm-14 cells were incubated with the increasing concentrations of G749 or AC220 and each indicated concentration of FLT3 ligand (FL). ATPLite assay was carried out after 48 hr incubation to determine cell viability. The IC₅₀ values were tabulated below the graphs. Note that gradual increment of FL concentration is correlated with that of cell viability. The exogenous addition of high FL concentration could reduce the potency of G-749 and AC220.

Supplementary Figure 9



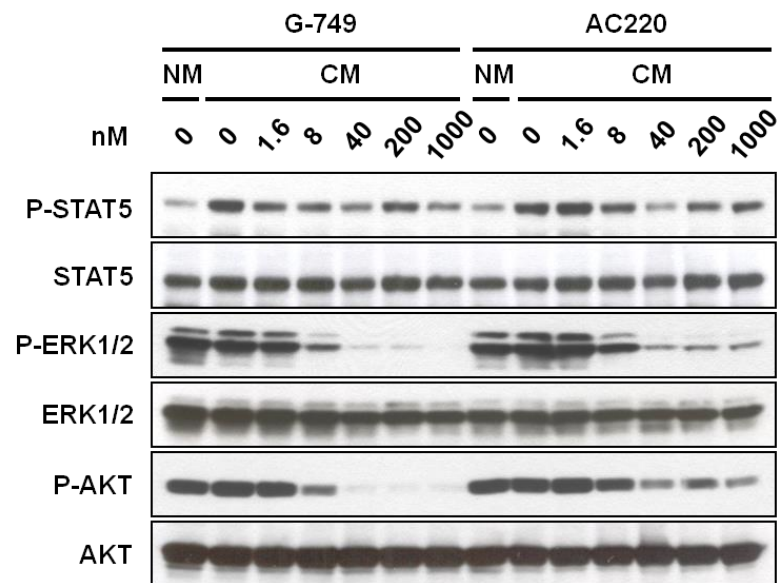
Supplementary Figure 9. Related Figure 1. Inhibition of FLT3 autophosphorylation in normal human plasma. MV4-11 cells were cultured in 100% human plasma with the indicated concentrations of FLT3 inhibitors for 2 hr. After cell lysis, phosphorylation of FLT3 was detected by ELISA. The absorbance values were normalized as percentage of DMSO-treated control. G-749, AC220 and PKC412 inhibited FLT3 autophosphorylation with IC_{50} value of 9.9, 52.8 and >1000 nM, respectively. Note that human plasma protein binding rate of G-749 and AC220 was 99.6% and 98%, respectively and G-749 shows more potent inhibition against FLT3 autophosphorylation than AC220 and PKC412.

Supplementary Figure 10.



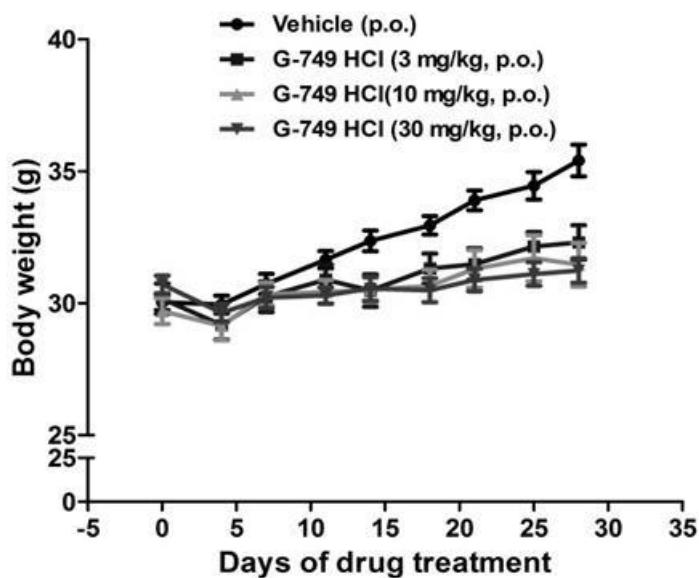
Supplementary Figure 10. MV4-11 cells were cocultured with HS-5 cells with the indicated inhibitors at 250 or 1000 nM 48 hr. Total cells were harvested and stained with FITC-Annexin V and PE-anti-CD45 antibody. Apoptotic CD45-positive cells were analyzed in a flow cytometry. CD45-negative cells were excluded in each dot plot to calculate the percentages of live and dead MV4-11 cells. Apoptotic population is distributed in the upper right of each dot plot.

Supplementary Figure 11.



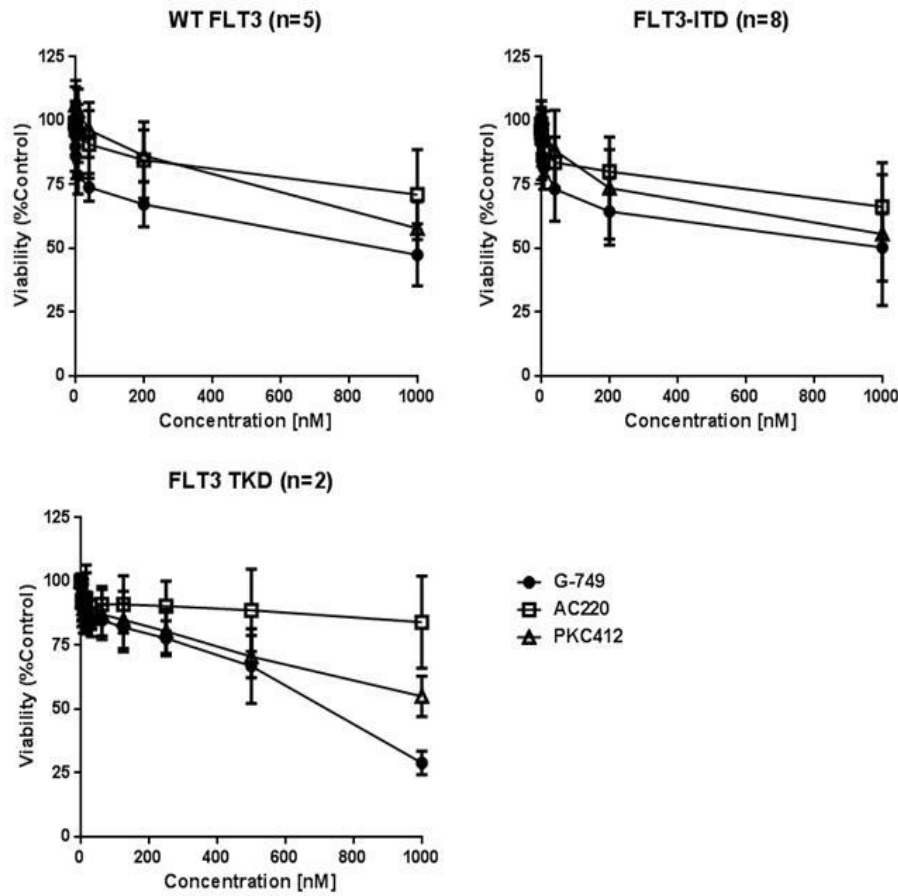
Supplementary Figure 11. Related Figure 4. Altered FLT3 downstream pathways in the conditioned medium (CM). MV4-11 cells were treated with the indicated concentrations of G-749 or AC220 in the presence or absence of HS-5-derived CM for 6 hr. The phosphorylation levels of downstream effectors, such as STAT5, AKT and ERK1/2, were then evaluated by immunoblotting. Note that AC220 in the CM did not fully inhibit phosphorylation of ERK1/2 and AKT at high concentrations but G-749 potently inhibited p-ERK1/2 and p-AKT. Both AC220 and G-749 did not inhibit p-STAT5.

Supplementary Figure 12.



Supplementary Figure 12. Related to Figure 5c. Body-weight of animals described in Figure 5c. The mice were weighed twice a week during measuring tumor size and plotted over days. The Error bars represent SEM.

Supplementary Figure 13.



Supplementary Figure 13. Related to Figure 6a. Integrated inhibitory activity of FLT inhibitors against patient blasts per each genotype, FLT3-wild type, FLT3-ITD or FLT3-TKD (D835Y). The patient bone marrow blasts were incubated with increasing concentrations of G-749, AC220 or PKC412 for 72 hr, and then their viability was determined by ATPLite assay. The data of patient(s) with wild type (n=5), those with FLT3-ITD (n=8) and those with FLT3-D835Y (n=2) were integrated. For each FLT3 inhibitor, the percentage over DMSO control was presented as a mean value, with error bars representing \pm s.d.

Supplementary Tables

Supplementary Table 1.

Kinase	IC ₅₀ , nM
FLT3	1
FLT3 (D835Y)	1
Mer	1
Aurora B	6
Ret	9
FLT1	18
Fms	19
Axl	20
Aurora C	24
FGFR1	25
FGFR3	30
KDR	39
c-Kit	142
IGF-1R	> 300
PDGFR α	>300
PDGFR β	>300
EGFR	>300

Supplementary Table 1. Kinase list inhibited by G-749. The IC₅₀ values were obtained by Millipore IC₅₀ profiler service. The complete percent inhibition by 100 nM G-749 is shown in the Supplementary Table 3.

Supplementary Table 2. Kinase inhibitory profile of G-749. The 100 nM of G-749 was challenged against 282 kinases for profiling. The ATP K_m of each enzyme was used.

kinase	% Inhibition (@ 0.1 μ M)
Abl(h)	0
Abl (H396P) (h)	5
Abl (M351T)(h)	11
Abl (Q252H) (h)	4
Abl(T315I)(h)	1
Abl(Y253F)(h)	28
ACK1(h)	33
ALK(h)	42
ALK4(h)	11
Arg(h)	9
AMPK α 1(h)	66
AMPK α 2(h)	69
ARK5(h)	83
ASK1(h)	6
Aurora-A(h)	57
Aurora-B(h)	97
Aurora-C(h)	70
Axl(h)	91
Blk(h)	46
Bmx(h)	36
BRK(h)	0
BrSK1(h)	50
BrSK2(h)	81
BTK(h)	2
BTK(R28H)(h)	9
CaMKI(h)	8
CaMKII β (h)	17
CaMKII γ (h)	66
CaMKI δ (h)	81
CaMKII δ (h)	72
CaMKIV(h)	31
CDK1/cyclinB(h)	39
CDK2/cyclinA(h)	19
CDK2/cyclinE(h)	43
CDK3/cyclinE(h)	33

kinase	% Inhibition (@ 0.1 μ M)
CDK5/p25(h)	72
CDK5/p35(h)	58
CDK6/cyclinD3(h)	20
CDK7/cyclinH (h)	30
CDK9/cyclin T1(h)	0
CHK1(h)	28
CHK2(h)	58
CHK2(I157T)(h)	42
CHK2(R145W)(h)	47
CK1 γ 1(h)	44
CK1 γ 2(h)	80
CK1 γ 3(h)	16
CK1 δ (h)	28
CK2(h)	0
CK2 α 2(h)	9
CLK2(h)	81
CLK3(h)	0
cKit(h)	29
cKit(D816V)(h)	39
cKit(D816H)(h)	97
cKit(V560G)(h)	91
cKit(V654A)(h)	82
CSK(h)	0
c-RAF(h)	0
cSRC(h)	22
DAPK1(h)	0
DAPK2(h)	1
DCAMKL2(h)	2
DDR2(h)	4
DMPK(h)	8
DRAK1(h)	77
DYRK2(h)	0
eEF-2K(h)	0
EGFR(h)	0
EGFR(L858R)(h)	91
EGFR(L861Q)(h)	9
EGFR(T790M)(h)	0
EGFR(T790M,L858R)(h)	5
EphA1(h)	18
EphA2(h)	0

kinase	% Inhibition (@ 0.1 μ M)
EphA3(h)	22
EphA4(h)	0
EphA5(h)	1
EphA7(h)	8
EphA8(h)	3
EphB2(h)	10
EphB1(h)	0
EphB3(h)	0
EphB4(h)	2
ErbB4(h)	0
FAK(h)	4
Fer(h)	21
Fes(h)	24
FGFR1(h)	78
FGFR1(V561M)(h)	38
FGFR2(h)	39
FGFR2(N549H)(h)	55
FGFR3(h)	70
FGFR4(h)	1
Fgr(h)	72
Flt1(h)	95
Flt3(D835Y)(h)	99
Flt3(h)	100
Flt4(h)	99
Fms(h)	76
Fms(Y969C)(h)	59
Fyn(h)	44
GCK(h)	50
GRK5(h)	14
GRK6(h)	0
GRK7(h)	0
GSK3 α (h)	1
GSK3 β (h)	0
Haspin(h)	34
Hck(h)	0
Hck(h) activated	56
HIPK1(h)	0
HIPK2(h)	7
HIPK3(h)	0
IGF-1R(h)	10

kinase	% Inhibition (@ 0.1 μ M)
IGF-1R(h), activated	59
IKK α (h)	2
IKK β (h)	0
IR(h)	17
IR(h), activated	74
IRR(h)	55
IRAK1(h)	17
IRAK4(h)	0
Itk(h)	21
JAK2(h)	0
JAK3(h)	0
JNK1 α 1(h)	0
JNK2 α 2(h)	0
JNK3(h)	14
KDR(h)	61
Lck(h)	17
Lck(h) activated	37
LIMK1(h)	4
LKB1(h)	3
LOK(h)	62
Lyn(h)	67
MAPK1(h)	0
MAPK2(h)	0
MAPKAP-K2(h)	0
MAPKAP-K3(h)	7
MEK1(h)	8
MARK1(h)	21
MELK(h)	92
Mer(h)	100
Met(h)	0
Met(D1246H)(h)	7
Met(D1246N)(h)	0
Met(M1268T)(h)	18
Met(Y1248C)(h)	4
Met(Y1248D)(h)	15
Met(Y1248H)(h)	15
MINK(h)	1
MKK6(h)	0
MKK7 β (h)	0
MLCK(h)	20

kinase	% Inhibition (@ 0.1 μ M)
MLK1(h)	29
Mnk2(h)	14
MRCK α (h)	0
MRCK β (h)	7
MSK1(h)	9
MSK2(h)	20
MSSK1(h)	6
MST1(h)	75
MST2(h)	57
MST3(h)	41
mTOR(h)	0
mTOR/FKBP12(h)	0
MuSK(h)	44
NEK2(h)	0
NEK3(h)	0
NEK6(h)	0
NEK7(h)	6
NEK11(h)	23
NLK(h)	9
p70S6K(h)	13
PAK2(h)	8
PAK4(h)	45
PAK5(h)	37
PAK6(h)	0
PAR-1B α (h)	15
PASK(h)	0
PEK(h)	0
PDGFR α (h)	17
PDGFR α (D842V)(h)	93
PDGFR α (V561D)(h)	87
PDGFR β (h)	9
PDK1(h)	67
PhK γ 2(h)	51
Pim-1(h)	0
Pim-2(h)	19
Pim-3(h)	0
PKA(h)	0
PKB α (h)	0
PKB β (h)	22
PKB γ (h)	0

kinase	% Inhibition (@ 0.1 μ M)
PKC α (h)	9
PKC β I(h)	6
PKC β II(h)	5
PKC γ (h)	9
PKC δ (h)	5
PKC ϵ (h)	0
PKC η (h)	0
PKC ι (h)	2
PKC μ (h)	0
PKC θ (h)	3
PKC ζ (h)	0
PKD2(h)	3
PKG1 α (h)	3
PKG1 β (h)	8
Plk1(h)	0
Plk3(h)	0
PRAK(h)	0
PRK2(h)	21
PrkX(h)	0
PTK5(h)	22
Pyk2(h)	48
Ret(h)	87
Ret (V804L)(h)	96
Ret(V804M)(h)	96
RIPK2(h)	0
ROCK-I(h)	0
ROCK-II(h)	4
ROCK-II(r)	8
Ron(h)	11
Ros(h)	3
Rse(h)	42
Rsk1(h)	66
Rsk1(r)	66
Rsk2(h)	59
Rsk3(h)	0
Rsk4(h)	1
SAPK2b(h)	0
SAPK3(h)	0
SAPK4(h)	0
SGK(h)	0

kinase	% Inhibition (@ 0.1 μ M)
SGK2(h)	1
SGK3(h)	8
SIK(h)	43
Snk(h)	8
Src(1-530)(h)	51
Src(T341M)(h)	78
SRPK1(h)	0
SRPK2(h)	0
STK33(h)	8
Syk(h)	0
TAK1(h)	0
TAO1(h)	20
TAO2(h)	15
TAO3(h)	8
TBK1(h)	14
Tec(h) activated	-2
TGFBR1(h)	0
Tie2 (h)	0
Tie2(R849W)(h)	9
Tie2(Y897S)(h)	12
TLK2(h)	1
TrkA(h)	94
TrkB(h)	90
TSSK1(h)	65
TSSK2(h)	18
Txk(h)	28
ULK2(h)	5
ULK3(h)	48
WNK2(h)	4
WNK3(h)	4
VRK2(h)	9
Yes(h)	75
ZAP-70(h)	0
ZIPK(h)	9

Sample no.	Age/Sex	FAB subclass	BM Cellularity (%)	FLT3 status WT/ITD/TKD	Karyotype	Status
1	27/M	MDS related AML	11 ~ 20	WT	46,XY,del(11)(p13p15)[19]/46,XY[1]	Remission
2	79/F	MDS related AML	51 ~ 60	WT	46,XX[20]	Relapsed
3	22/M	M5b	61 ~ 70	WT	46,XY,t(8;21)(q22;q22)[16]/46,XY[1]	Remission
4	77/F	M5a	21 ~ 30	WT	46,XX[20]	Remission
5	54/F	M5	71 ~ 80	WT	47,XX,inv(16)(p13.1q22),+22[20]	Remission
6	22/F	M2	11 ~ 20	WT	46,XX[20]	Remission
7	45/M	M3	91 ~ 100	WT	46,XY[6]	Remission
8	66/M	M3	61 ~ 70	WT	46,XY,t(8;21)(q22;q22)[10]	Remission
9	62/F	M1	51 ~ 60	WT	46~48,XX,+8,+1~2mar.inc[cp11]	Relapsed
10	62/M	M4	41 ~ 50	WT	46,XY[12]	Relapsed

Supplementary Table 3. Related Figure 3b and 3c. The information of bone marrow plasmas from AML patients after induction therapy with Cytarabine.

Abbreviations: FAB, French–American–British; MDS, myelodysplastic syndromes; FLT3, FMS-like receptor tyrosine kinase 3; WT, wild type; ITD, internal tandem duplications; TKD, tyrosine kinase domain.

Sample no.	Age/Sex	FAB subclass	Blasts initial PB%	FLT3 status WT/ITD/TKD	Karyotype	Status
1	75/F	M2	80%	WT	46,XX	Diagnostic
2	66/F	M1	43%	WT	46,XY	Diagnostic
3	71/F	M1	79%	WT	46,XX	Diagnostic
4	73/M	M2	45%	WT	46,XY	Diagnostic
5	69/M	M2	20%	WT	46,XY	Diagnostic
6	66/M	M1	15%	ITD	46,XY	Diagnostic
7	57/M	M2	65%	ITD	ND	Diagnostic
8	61/F	M2	10%	ITD	46,XX	Diagnostic
9	18/F	M4	ND	ITD	ND	Diagnostic
10	25/M	M1	93%	ITD	46,XY	Diagnostic
11	22/M	M1	95%	ITD	ND	Diagnostic
12	22/M	M5	55%	ITD	46,XY	Relapsed
13	38/F	M1	87%	TKD (D835Y)	46,XX,t(6;11)(q27;q23)	Diagnostic
14	34/M	M3	86%	TKD (D835Y)	46,XY,t(15;17)(q22;q12)	Diagnostic
15	53/M	M3	97%	ITD	46,XY,t(15;17)(q22;q12)	Diagnostic
16	38/M	M3	90%	ITD/TKD (D835Y)	46,XY,t(15;17)(q22;q12)	Diagnostic

Supplementary Table 4. Related Figure 6a and 6b. The information of bone marrow blasts from patients diagnosed as acute myeloid leukemia and their FLT3 mutation status. Abbreviations: FAB, French–American–British; FLT3, FMS-like receptor tyrosine kinase 3; WT, wild type; ITD, internal tandem duplications; TKD, tyrosine kinase domain; ND, not done.